Electronic Supplementary Information

Swinging molecular adsorption of carbon monoxide on ferroelectric $BaTiO_3(001)$

Alexandru-Cristi Iancu,[a,b] Nicoleta G. Apostol,[a] Adela Nicolaev,[a] Laura E. Abramiuc,[a] Cristina F. Chirilă,[a] Dana G. Popescu,[a] and Cristian M. Teodorescu[a,*]

[a]National Institute of Materials Physics, Atomiștilor 405A, 077125 Măgurele, Ilfov, Romania
[b]University of Bucharest, Faculty of Physics, Atomiștilor 405, 077125 Măgurele, Ilfov, Romania

*corresponding author, e-mail teodorescu@infim.ro

X-ray diffraction and X-ray reflectivity

The structure and morphology of the deposited BTO film were investigated using X-ray diffraction (XRD, Figure S1) and the thickness was estimated using X-ray reflectivity (XRR, Figure S2). The measurements (2θ–ω scans in the 2θ range from 15 to 80° with 0.02° step and 1 degree per minute scan speed) were performed using a Rigaku SmartLab diffractometer equipped with high-resolution optics in parallel beam (a double monochromator Ge(220) in the incident beam) and a Hypix detector in 0D regime. For the asymmetric reciprocal space map (RSM) a BRUKER D8 Advance diffractometer was used, in parallel beam, without a monochromator. Both diffractometers used a X-ray source with Cu anode, powered at 40 kV and 40 mA.

The XRD results of the BTO/STON sample are prezented in Figure S1. Collecting symmetric 2θ–ω scans we can investigate the out-of-plane lattice parameter (c = 4.121 Å) and demonstrate the high crystalline quality of the samples. The most intense peaks correspond to $00l$ lines of the tetragonal BTO film (c/a = 1.055) and cubic STON substrate, showing the orientation of (001) film planes parallel to the (001) planes of the substrate (BTO (001)//STON (001)).

In order to quantify the lattice constants of the sample the RSM was performed. The inset in Figure S1 shows scans around the asymmetric $(\bar{1}03)$ nodes of the STON substrate in the reciprocal space of the BTO thin film. The in-plane latice constant a = 3.905 Å indicate a fully strained film (V_{cell} = 62.841 Å^3).

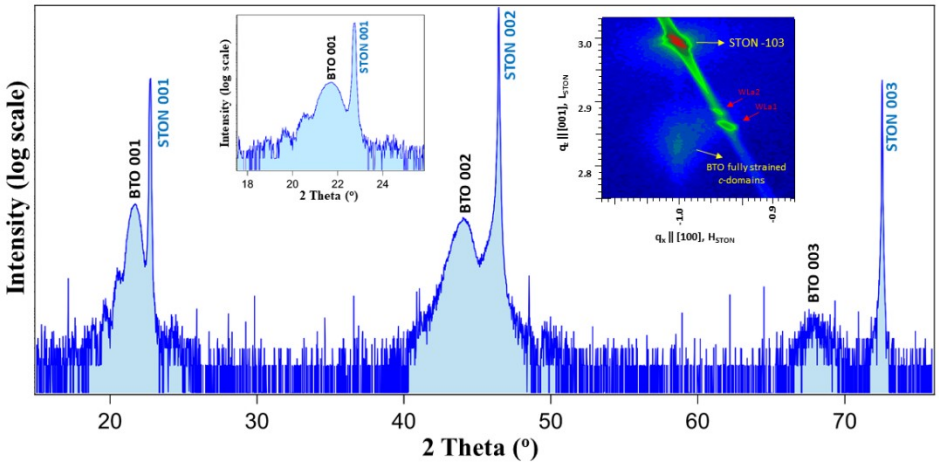

Figure S1: The XRD pattern of the BTO/STON sample, showing in the insets details around the 001 lines of the substrate and the reciprocal space mapping in the vicinity of -103 node of the STON substrate.

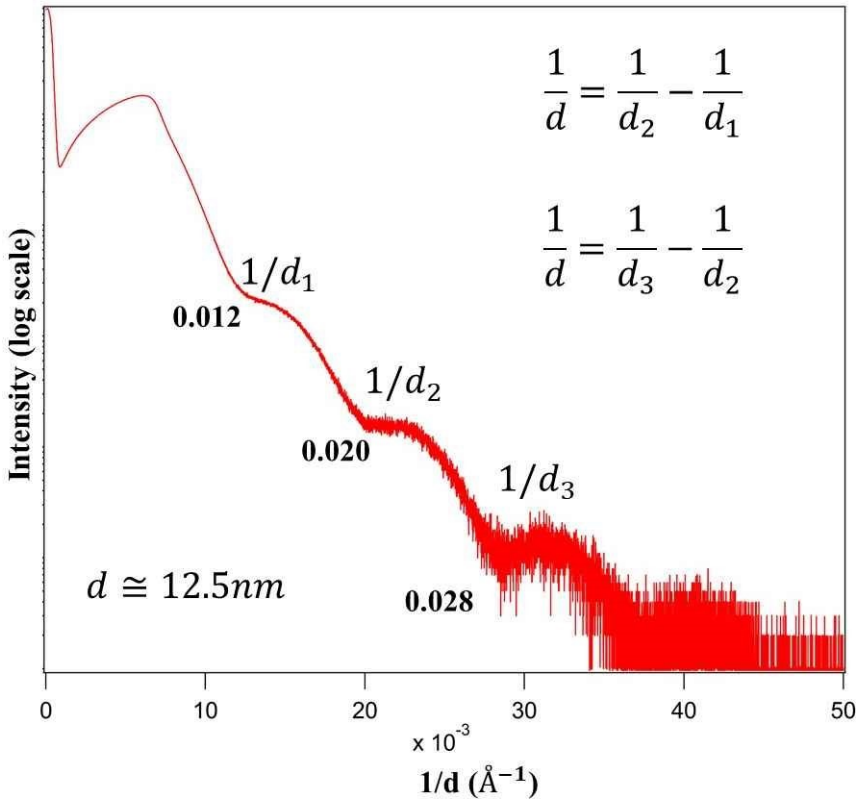

Figure S2. X-ray reflectivity measurement of BTO(001), together with the derivation procedure of the film thickness.

X-ray reflectivity (Figure S2) was performed in parallel beam geometry using a 0D detector, from 0°–8° with a 0.01° step and 1 degree per minute scan speed.

Survey XPS spectra

Figure S3 (next page). Survey XPS spectra for two clean BTO(001) surfaces and after three CO dosing (3.4 kL) at different temperatures.

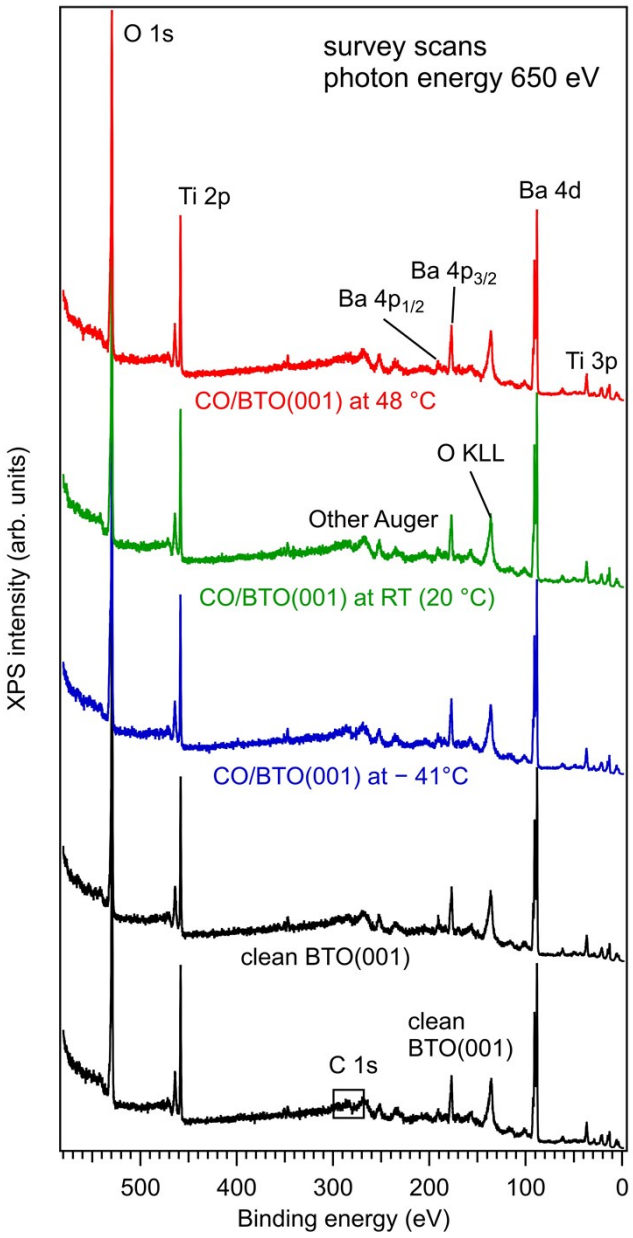

Ti 2p XPS spectra obtained with monochromatic Al K_α radiation

Figure S4 (next page). Ti 2p XPS spectra obtained with monochromatic Al K_α radiation, for a 'as introduced' BTO(001) (a) and after the cleaning procedure (b), with 'deconvolutions' similar to those described in the main text.

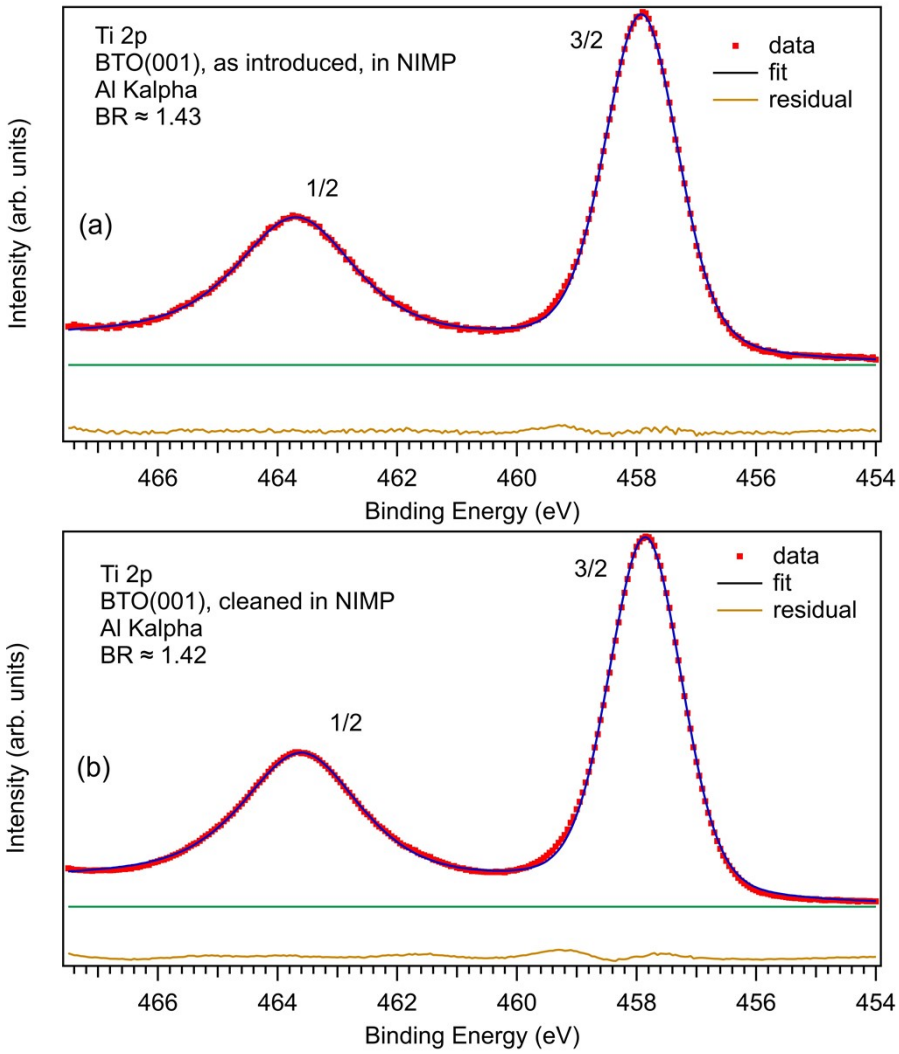

Derivation of inelastic mean free paths by using uncorrected Ti 2p intensity

The correction factor introduced in the main text for the 'lost' intensity supposed for the Ti $2p_{3/2}$ peak was not considered in the simulation whose results are represented below. The procedure is the same as that described in the main text. For survey, the ratios considered are $I_{Ba}/I_{Ti} \approx 3.62$ and $I_O/I_{Ba} \approx 1.45$. For bulk components, the ratios considered are $I^{bulk}_{Ba}/I^{bulk}_{Ti} \approx 1.81$ and $I^{bulk}_{O}/I^{bulk}_{Ba} \approx 1.72$. From Fig. S5 one may notice that there is a discrepancy between the solutions λ_{Ti} obtained from the intersections of $\lambda_{Ba}(\lambda_{Ti})$ and $\lambda_O(\lambda_{Ti})$ (in c units) from the evaluation of total peak intensities (from survey spectra) and from the bulk components (from the results of peak fit analysis). Also, the value $\lambda_{Ti}/c = 0.54\ and\ 0.61$ (2.2 to 2.5 Å) obtained from the intersection of two families of solutions is far too low to be credible.

Figure S5 (next page). Results of the Monte-Carlo simulation yielding sets of inelastic mean free (IMFP) path values for Ba 4d, O 1s and Ti 2p (photon energy 650 eV), from the analysis of total XPS intensities (survey spectra), red symbols, and from the analysis of the 'bulk' components from 'deconvoluted' spectra, blue symbols. The IMFPs of Ba and O divided by the lattice parameter *c* are plotted vs. the IMFP of Ti divided by *c*. Straight lines are linear fits.

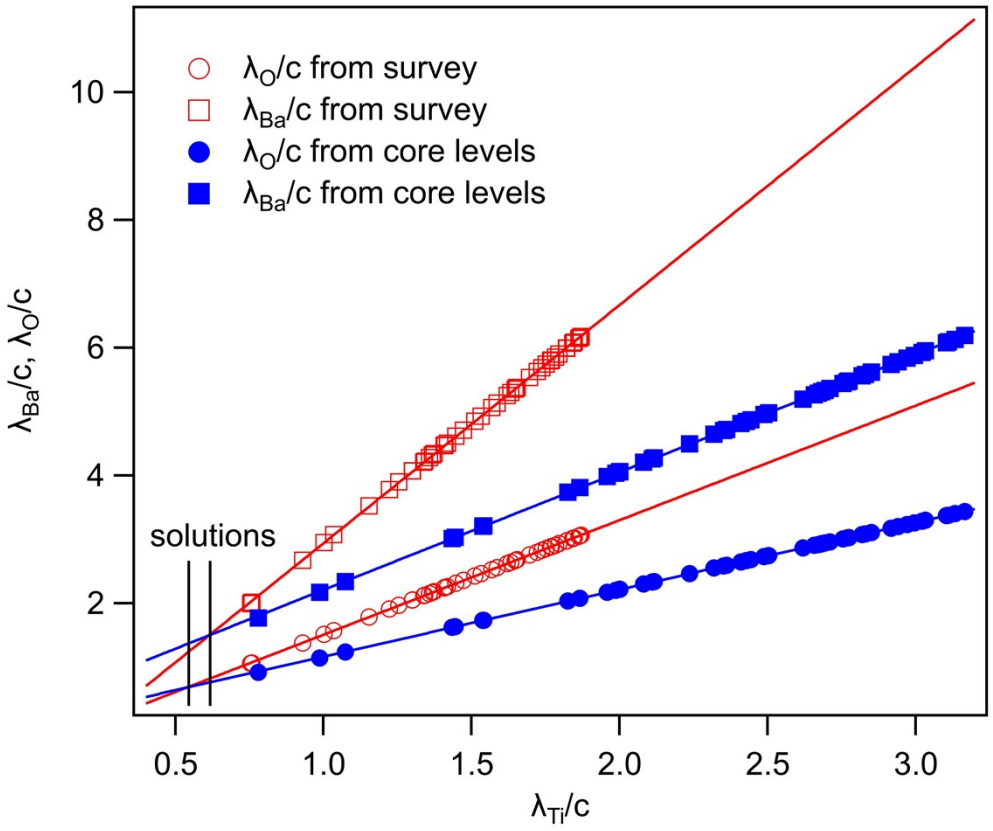

Transitions from Ti $2p_{1/2}$ and Ti $2p_{3/2}$ core levels, together with their relative weight

Figure S6 (next page). Photoionization transitions from several states from $2p_{1/2}$ (a_1, a_2) and $2p_{3/2}$ (b_1, b_2, b_3) core levels towards continuum states characterized by the energy ε and several values of the total angular moment and of its projections. For each transition, the squared value of the corresponding Clebsch-Gordan coefficient is given, by observing the color code for the transition in question.

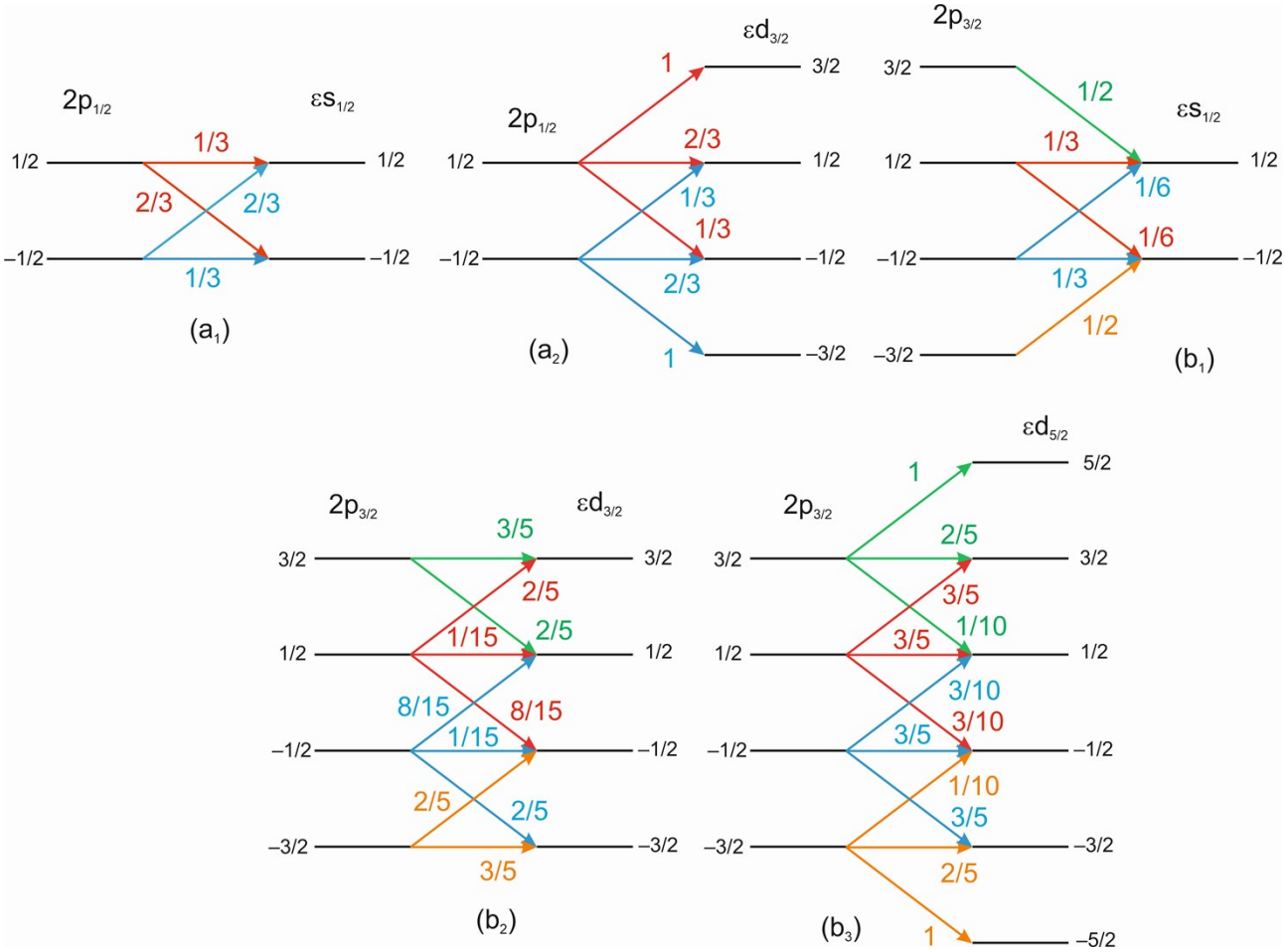

TPD data after CO adsorption at room and at high temperature

Figure S7 (next page). Temperature-programmed desorption of CO initially adsorbed at room or high temperature (3.5 kL), follow-up using all core levels: (a) Ba 4d; (b) Ti 2p; (c) O 1s; (d) C 1s. Dots are experimental data (red lines for C 1s). Full lines are fitting functions (black for the total fit) and separate contribution of two ‘components’ (for Ba 4d and O 1s). For fits, similar functions as for the basic XPS analysis from Fig. 3 are used, just for O 1s only two Voigt singlets instead of three were employed. The results of the simulation are captured in Figure 8 together with that of the desorption following adsorption at low temperature, Figure 7, main text.

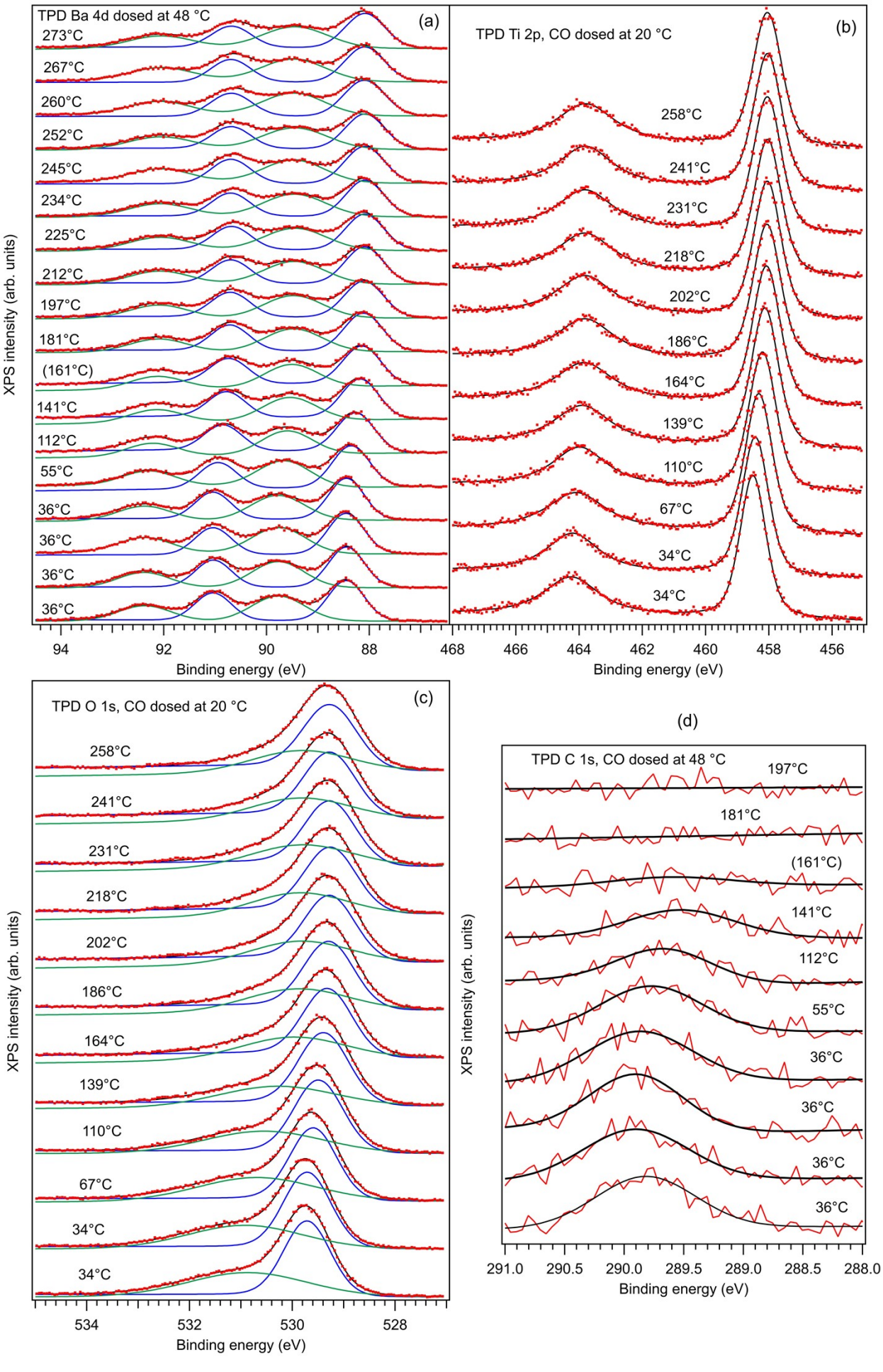
TPD Ba 4d dosed at 48 °C
(a)
273°C
267°C
260°C
252°C
245°C
234°C
225°C
212°C
197°C
181°C
(161°C)
141°C
112°C
55°C
36°C
36°C
36°C
36°C
XPS intensity (arb. units)
94
92
90
88
Binding energy (eV)
TPD Ti 2p, CO dosed at 20 °C
(b)
258°C
241°C
231°C
218°C
202°C
186°C
164°C
139°C
110°C
67°C
34°C
34°C
468
466
464
462
460
458
456
Binding energy (eV)
TPD O 1s, CO dosed at 20 °C
(c)
258°C
241°C
231°C
218°C
202°C
186°C
164°C
139°C
110°C
67°C
34°C
34°C
XPS intensity (arb. units)
534
532
530
528
Binding energy (eV)
(d)
TPD C 1s, CO dosed at 48 °C
197°C
181°C
(161°C)
141°C
112°C
55°C
36°C
36°C
36°C
36°C
XPS intensity (arb. units)
291.0
290.5
290.0
289.5
289.0
288.5
288.0
Binding energy (eV)

C 1s evolution with soft X-ray irradiation

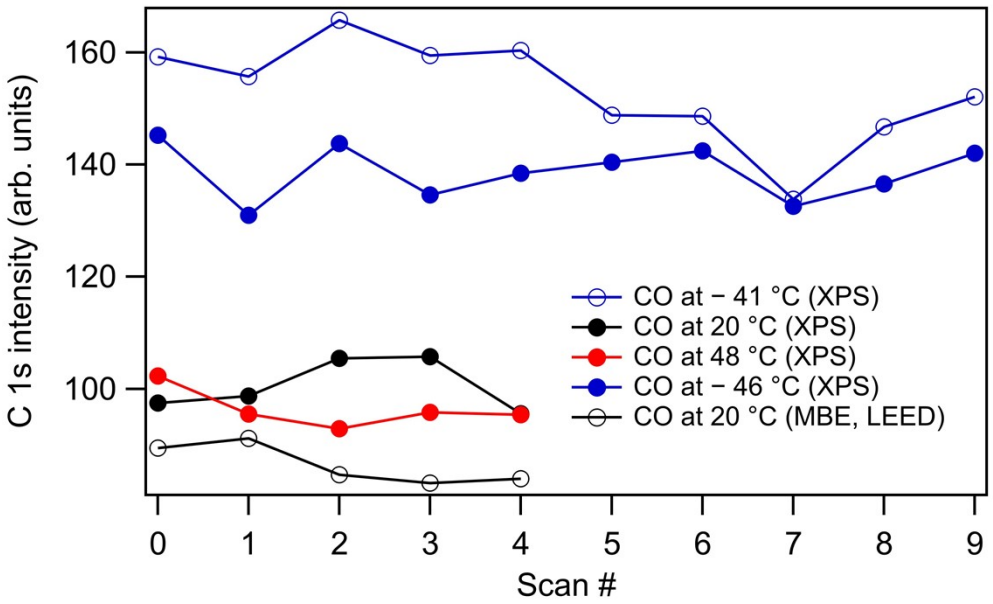

Figure S8. Evolution of the integral intensity of the C 1s intensity, obtained by fitting individual scans of C 1s spectra with a gaussian, as soon as the CO dosing was terminated and the sample was irradiated with soft X-rays at 390 eV photon energy. One scan lasts about one minute. Data are represented for several CO dosing in different conditions. Most dosing were performed in the XPS chamber, but there was also a dosing in the MBE chamber at room temperature, when the LEED experiments before and after dosing were performed.